RSC Advances

PAPER

View Article Online
View Journal | View Issue

Cite this: *RSC Adv.*, 2017, **7**, 19073

New discrete iodometallates with *in situ* generated triimidazole derivatives as countercations (M^{n+} = Ag^{+}, Pb^{2+}, Bi^{3+})†

Rong-Yan Wang,[a] Xiao Zhang, *[b] Qi-Sheng Huo,[a] Jie-Hui Yu *[a] and Ji-Qing Xu[a]

Through employing the solvothermal *in situ N*-alkylation of organic bases with alcohol molecules, four new iodometallates $[L1]_2[Ag_8I_{12}]I_2$ ($L1^{3+}$ = 1,1′,1″-(benzene-1,3,5)tris(3-methyl-1*H*-imidazol-3-ium)) **1**, $[L1]_2[Ag_6I_{12}]$ **2**, $[L1]_2[Pb_3I_{12}]\cdot 2H_2O$ **3**, and $[L1][Bi_2I_9]$ **4** were obtained. $L1^{3+}$ originates from the *in situ N*-alkylation between 1,3,5-tri(1*H*-imidazol-1-yl)benzene (L2) and CH_3OH. X-ray single-crystal diffraction analysis reveals that all of the title compounds possess zero-dimensional (0D) structures. The octanuclear anionic cluster $[Ag_8I_{12}]^{4-}$ of **1** possesses a sphere-like structure. An Ag_6I_6 unit with a hexagram structure occupies the equatorial position, while two AgI_4 tetrahedra (sharing point) occupy the axial positions. The anionic cluster, $[Ag_6I_{12}]^{6-}$, of **2** exhibits a hexanuclear structure, which can be described as an aggregation of two incomplete cubanes (each lacking an Ag^{+} corner). The anionic cluster $[Pb_3I_{12}]^{6-}$ of **3** can be described as an aggregation of three PbI_6 octahedra (sharing face), whereas two BiI_6 octahedra (also sharing face) aggregate to form a dinuclear cluster $[Bi_2I_9]^{3-}$ of **4**.

Received 29th November 2016
Accepted 24th March 2017

DOI: 10.1039/c6ra27510a

rsc.li/rsc-advances

Introduction

As a new high-efficiency synthetic approach, the *in situ* ligand preparation approach has seen rapid development in the last two decades.[1] The *in situ* ligand synthesis approach not only simplifies the reactive procedure, but also creates a variety of new organic molecules and complexes. A majority of ligand *in situ* reactions originate from accidental discovery. Then they are extensively employed in the construction of new organic molecules and complexes. Finally, it becomes a classical reaction. So far, the typical ligand *in situ* reactions are the cycloaddition of organic nitriles with azide,[2] oxidative hydroxylation of aromatic rings,[3] dehydrogenative coupling of C–C bonds,[4] acylation of multicarboxylic acids with N_2H_4,[5] *N*-alkylation of heterocyclic ligands with alcohols, and so on.[6]

The *in situ N*-alkylation of organic bases with alcohol molecule was discovered for the first time when preparing compound $[CH_3CH_2S\text{-}4\text{-}C_5H_4N\text{–}CH_2CH_3][Cu_3I_4]$.[7] The *N*-alkylation between CH_3CH_2S-4-C_5H_4N and C_2H_5OH solvent occurred to generate $CH_3CH_2S\text{-}4\text{-}C_5H_4N^{+}\text{–}CH_2CH_3$. Latter, the researchers employed this kind of *in situ* reaction to construct many new hybrid organic–inorganic materials.[8] For example, Lang *et al.* employed the *in situ N*-alkylation of 4-cynaopyridine (4-cypy) or 4,4′-bipyridine (4,4′-bpy) with various alcohols to prepare a serials of hybrid iodometallates [M^{n+} = Cu^{+}, Pb^{2+}, Bi^{3+}].[9] Guo *et al.* employed the *in situ N*-alkylation of aromatic diamines or 1,4-diazabicyclo[2,2,2]octane (dabco) with diverse alcohols to construct a serials of hybrid iodoplubates.[10] Zhang *et al.* employed the *in situ N*-alkylation of pyridine (py), 4,4′-bpy, 1,3-bis(4-pyridyl)propane (bpp), or dabco with CH_3OH or C_2H_5OH to create some iodocuprate(I) and bromocuprate(I).[11] Wang *et al.* utilized the *N*-alkylation of piperazine (pip), pip derivatives, dabco or 3-(aminomethyl)pyridine (ampy) with CH_3OH to synthesize a series of metal phosphates and phosphites (M^{n+} = Be^{2+}, Ga^{3+}, Zn^{2+}).[12] In the past, our group also employed this kind of *in situ* reaction to construct some iodocuprates(I) and iodoplumbates(II).[13] The used organic bases have pip, dabco, 4,4′-bipiperidine (bp), 1,3-bis(4-piperidyl) propane (bpip) and py. Even though the *in situ N*-alkylation of so many organic bases (cyclic aliphatic organic bases, aromatic bisamine, py/derivatives) have been investigated, the triimidazole molecules are never considered. In this article, the *in situ N*-alkylation of 1,3,5-tri(1*H*-imidazol-1-yl)benzene (L2) with alcohols are investigated, and four new iodometallates as the octanuclear $[L1]_2[Ag_8I_{12}]I_2$ ($L1^{3+}$ = 1,1′,1″-(benzene-1,3,5)tris(3-methyl-1*H*-imidazol-3-ium)) **1**, hexanuclear $[L1]_2[Ag_6I_{12}]$ **2**, trinuclear $[L1]_2[Pb_3I_{12}]\cdot 2H_2O$ **3**, and the dinuclear $[L1][Bi_2I_9]$ **4** were obtained. $L1^{3+}$ originated from the solvothermal *in situ N*-alkylation of L2 with CH_3OH.

[a]*College of Chemistry, State Key Laboratory of Inorganic Synthesis and Preparative Chemistry, Jilin University, Changchun, Jilin, 130012, China. E-mail: jhyu@jlu.edu.cn*
[b]*MIIT Key Laboratory of Critical Materials Technology for New Energy Conversion and Storage, School of Chemistry and Chemical Engineering, Harbin Institute of Technology, Harbin, 150080, China. E-mail: Zhangx@hit.edu.cn*

† Electronic supplementary information (ESI) available. CCDC 1519637–1519640. For ESI and crystallographic data in CIF or other electronic format see DOI: 10.1039/c6ra27510a

Experimental

General

All chemicals are of reagent grade quality, obtained from commercial sources without further purification. Elemental analysis (C, H and N) was performed on a Perkin-Elmer 2400LS II elemental analyzer. Infrared (IR) spectrum was recorded on a Perkin Elmer Spectrum 1 spectrophotometer in 4000–400 cm^{-1} region using a powdered sample on a KBr plate. Powder X-ray diffraction (XRD) data were collected on a Rigaku/max-2550 diffractometer with Cu-K_α radiation (λ = 1.5418 Å). Thermogravimetric (TG) behavior was investigated on a Perkin-Elmer TGA-7 instrument with a heating rate of 10 °C min^{-1} in air. Ultraviolet-visible (UV-vis) spectrum was obtained on a Rigaku-UV-3100 spectrophotometer.

Synthesis of title compounds

$[L1]_2[Ag_8I_{12}]I_2$ 1. The yellow columnar crystals of **1** were obtained from a simple solvothermal self-assembly of AgI (12 mg, 0.05 mmol), L2 (28 mg, 0.1 mmol), and HI (45%, 1 mL) in a mixed solvent of CH_3CN (4 mL) and CH_3OH (2 mL) (pH = 2) at 110 °C for 3 days. Yield: *ca.* 24% based on Ag(I). Anal. calcd $C_{36}H_{42}N_{12}Ag_8I_{14}$ **1**: C 13.17, H 1.29, N 5.12. Found: C 13.22, H 1.33, N 5.23%. IR (cm^{-1}): 3086 m, 3051 m, 2925 w, 2849 w, 1614 s, 1575 s, 1419 w, 1386 w, 1239 w, 1190 s, 862 w, 809 s, 747 s, 673 s, 614 s.

$[L1]_2[Ag_6I_{12}]$ 2. The yellow columnar crystals of **2** were obtained from a simple solvothermal self-assembly of AgBr (19 mg, 0.05 mmol), L2 (28 mg, 0.1 mmol), and HI (45%, 1 mL) in a mixed solvent of CH_3CN (6 mL) and CH_3OH (2 mL) (pH = 2) at 120 °C for 3 days. Yield: *ca.* 31% based on Ag(I). Anal. calcd $C_{36}H_{42}N_{12}Ag_6I_{12}$ **2**: C 15.37, H 1.51, N 5.98. Found: C 15.51, H 1.65, N 5.78%. IR (cm^{-1}): 3063 w, 3034 w, 2920 w, 2854 w, 1637 m, 1618 s, 1386 w, 1194 m, 1135 w, 816 w, 614 s.

$[L1]_2[Pb_3I_{12}]\cdot 2H_2O$ 3. The yellow columnar crystals of **3** were obtained from a simple solvothermal self-assembly of PbI_2 (46 mg, 0.1 mmol), L2 (14 mg, 0.05 mmol), and HI (45%, 1 mL) in a mixed solvent of CH_3CN (8 mL) and CH_3OH (2 mL) (pH = 2) at 110 °C for 3 days. Yield: *ca.* 46% based on Pb(II). Anal. calcd $C_{36}H_{46}N_{12}O_2Pb_3I_{12}$ **3**: C 15.31, H 1.64, N 5.95. Found: C 15.42, H 1.61, N 6.02%. IR (cm^{-1}): 3091 w, 3043 w, 2919 w, 2853 w, 1637 m, 1617 s, 1545 w, 1386 w, 1190 s, 1135 w, 871 w, 818 m, 671 w, 613 s.

$[L1][Bi_2I_9]$ 4. The red columnar crystals of **4** were obtained from a simple solvothermal self-assembly of $BiCl_3$ (32 mg, 0.05 mmol), L2 (28 mg, 0.1 mmol), and HI (45%, 1 mL) in a mixed solution of CH_3CN (6 mL) and CH_3OH (2 mL) (pH = 2) at 110 °C for 3 days. Yield: *ca.* 39% based on Bi(III). Anal. calcd $C_{18}H_{21}N_6Bi_2I_9$ **4**: C 14.49, H 1.13, N 4.47. Found: C 14.35, H 1.01, N 4.58%. IR (cm^{-1}): 3100 w, 3071 w, 2929 w, 2853 w, 1623 s, 1587 s, 1548 s, 1418 w, 1385 w, 1348 w, 1208 s, 1110 w, 1087 m, 855 m, 813 s, 768 m, 680 w, 611 s.

The title four hybrids are stable in air, and soluble in H_2O, methanol, ethanol, acetone and acetonitrile.

X-ray crystallography

The data were collected with Mo-K_α radiation (λ = 0.71073 Å) on a Rigaku R-AXIS RAPID IP diffractometer for **1**, **3** and **4**, and on a Siemens SMART CCD diffractometer for **2**. With SHELXTL program, the structures of **1–4** were solved using direct methods.[14] The non-hydrogen atoms were assigned anisotropic displacement parameters in the refinement, and the hydrogen atoms were treated using a riding model. The hydrogen atoms on the water molecule in **3** are not located. The structures were then refined on F^2 using SHELXL-97.[14] CCDC numbers are 1519637–1519640 for **1–4**, respectively. The crystallographic data for **1–4** are summarized in Table 1.

Table 1 Crystal data of title compounds

	1	2	3	4
Formula	$C_{36}H_{42}N_{12}Ag_8I_{14}$	$C_{36}H_{42}N_{12}Ag_6I_{12}$	$C_{36}H_{46}N_{12}O_2Pb_3I_{12}$	$C_{18}H_{21}N_6Bi_2I_9$
M	3282.38	2812.84	2823.22	1881.47
T (K)	293(2)	293(2)	293(2)	293(2)
Crystal system	Rhombohedral	Monoclinic	Monoclinic	Orthorhombic
Space group	$R\bar{3}$	$P2_1/c$	$P2_1/n$	$P2_12_12_1$
a (Å)	14.090(2)	11.2094(3)	12.496(3)	12.485(3)
b (Å)	14.090(2)	13.2371(4)	20.569(4)	13.080(3)
c (Å)	31.201(6)	21.8384(5)	12.634(3)	23.566(5)
α (°)	90	90	90	90
β (°)	90	92.965(2)	100.16(3)	90
γ (°)	120	90	90	90
V (Å^3)	5364.4(15)	3236.04(15)	3196.3(11)	3848.4(13)
Z	3	2	2	4
D_c (g cm^{-3})	3.048	2.887	2.933	3.247
μ (mm^{-1})	8.219	7.540	13.716	16.371
Reflections collected	17 338	18 068	30 245	37 053
Unique reflections	2739	5716	7292	8789
R_{int}	0.0504	0.0460	0.0870	0.0698
Gof	1.094	0.979	1.050	1.040
R_1, $I > 2\sigma(I)$	0.0417	0.0343	0.0492	0.0382
wR_2, all data	0.0954	0.0810	0.0926	0.0705

Results and discussion

Synthetic analysis

All of the title compounds were obtained under the solvothermal conditions. The reactions of metal halides (M^{n+} = Ag^{+}, Pb^{2+}, Bi^{3+}), L2 and HI in a mixed solvent (containing CH_3OH) at a strong acidic condition created the title compounds **1–4**. The *N*-alkylation of L2 with CH_3OH occurred to generate $L1^{3+}$ (see Scheme 1). The equations below show a potential reactive process: (i) $CH_3OH + HI = CH_3I + H_2O$; (ii) $L2 + 3CH_3I = L1I_3$. The second-step reaction can occur at an acidic or neutral environment, but the formation of CH_3I for the first-step reaction maybe needs a strong acidic environment. The other alcohol molecules as C_2H_5OH and C_3H_7OH were used to be in place of CH_3OH, but the IR spectrum analyses for the obtained solid samples reveal that the *N*-alkylation of L2 with these alcohols did not occur. The reaction using CuI as the metal resource was also carried out, but unfortunately, the crystal data of the product $[L1]_2[Cu_6I_{12}]$ did not pass the cif-checking examination. The reactions without the CH_3OH solvent were also investigated, and only a Pb^{2+} hybrid $[H_3L2][PbI_4]$ was obtained.

Structural description

$[L1]_2[Ag_8I_{12}]I_2$ 1. X-ray single-crystal diffraction analysis reveals that **1** is an octanuclear iodoargentate with $L1^{3+}$ as the countercation (see Fig. 1a). The asymmetric unit of **1** is found to be composed of two types of Ag^{+} ions (Ag1, Ag2), four types of I^{-} ions (I1, I2, I3, I4), and one $L1^{3+}$ molecule. Ag1 and Ag2 are both in a tetrahedral site with four I^{-} ions as the donor atoms (I1, I2, I2a and I3 for Ag1; I1, I1c, I1d and I3 for Ag2). The Ag–I distances span a quite wide range from 2.7704(6) Å to 3.1694(15) Å. For four types of I^{-} ions, I4 exists in a free form, while the other three I^{-} ions act as the bridging ligands. I1 and I2 adopt a simple double-bridged coordination mode, whereas I3 adopts a special μ_8 coordination mode. With $L1^{3+}$ as the counteraction, Ag^{+} and I^{-} aggregate to form an octanuclear cluster. This cluster possesses a sphere-like structure (see Fig. 1b). Six symmetry-related I2 ions bridge six symmetry-related Ag1 centers to form a hexagram, occupying the equatorial position of the sphere. Note that this hexagram is not planar. Six I^{-} ions are nearly co-planar with a minor mean deviation of 0.0852 Å. Three Ag^{+} ions are above the six iodine plane, while the other three Ag^{+} ions lie below the six iodine plane. Two $Ag(2)I_4$ tetrahedra occupy the axial positions. These two tetrahedra share the I3 ion. I3 lies at the center of the sphere. *Via* the Ag1–I1 and Ag1–I3 interactions, the Ag_6I_6 hexagram and two AgI_4 tetrahedral aggregate together to form the octanuclear anionic cluster of **1**. The shortest Ag···Ag separation in **1** is Ag1···Ag1a = 3.4455(10) Å. To the formation of this octanuclear cluster, the free I4 ion should play a key role.

$[L1]_2[Ag_6I_{12}]$ 2. Without the existence of the free I^{-} ion, Ag^{+} and I^{-} aggregate into a hexanuclear cluster. Here $L1^{3+}$ still serves as the countercation in **2** (see Fig. 2). The asymmetric unit of **2** is found to be composed of three types of Ag^{+} ions (Ag1, Ag2, Ag3), six types of I^{-} ions (I1, I2, I3, I4, I5, I6), and one $L1^{3+}$ molecule. Three Ag^{+} centers all exhibit a tetrahedral geometric configuration with an AgI_4 donor set. The Ag–I bond length range is 2.7512(9)–2.9597(9) Å. Six I^{-} ions adopt three types of coordination modes: terminal mode for I2 and I5; double-bridged mode for I1 and I3; triple-bridged mode for I4 and I6. The Ag–I–Ag angles for linear I1 and I3 are 67.93(2)° (for I1) and 78.41(3)° (for I3), respectively. Both I4 and I6 adopt a triple pyramidal geometrical configuration. However, the triple pyramid for I4 are regular, while the triple pyramid for I6 suffers from a severe distortion. It looks more like a slice of the rectangular pyramid (losing an Ag^{+} corner). The distances from the apical I^{-} ions to the three Ag^{+} planes are 2.33 Å (for I4) and 1.04 Å (for I6), respectively. Templated by $L1^{3+}$, a hexanuclear iodoargentate forms. Three I^{-} ions (I1, I3 and I6) first bridge alternately three Ag^{+} centers to form a trinuclear cluster. The I4

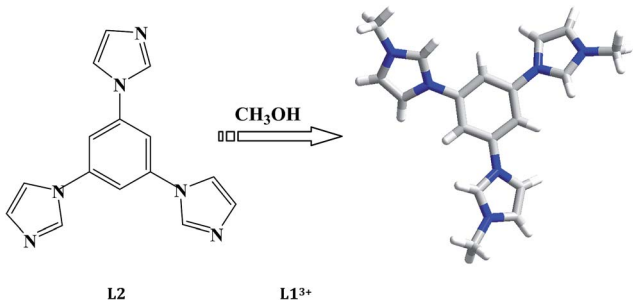

Scheme 1 *In situ* *N*-alkylation of L2 with CH_3OH into $L1^{3+}$.

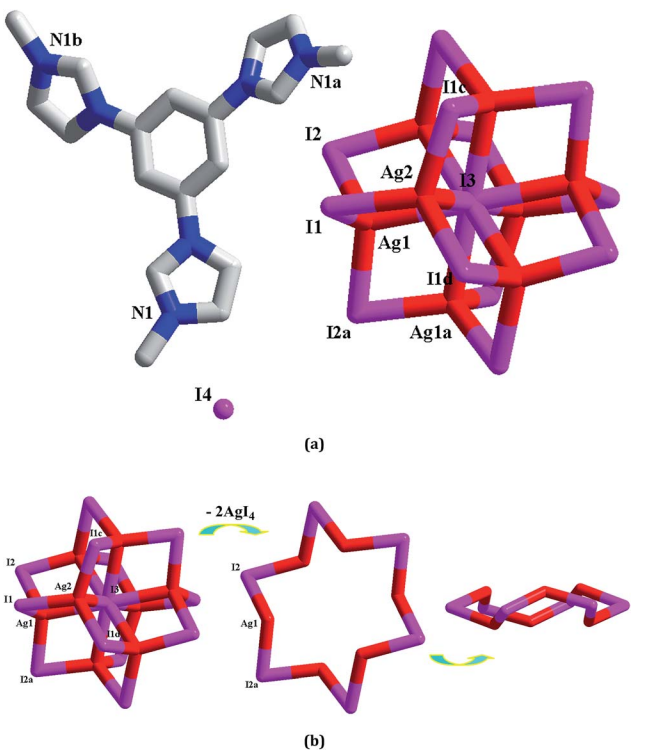

Fig. 1 Molecular structure (a) and anionic cluster structure (b) for **1** (*a*: $y - 1/3, -x + y + 1/3, -z + 1/3$; *b*: $x - y + 2/3, x + 1/3, -z + 1/3$; *c*: $-x + y, -x + 1, z$; *d*: $-y + 1, x - y + 1, z$).

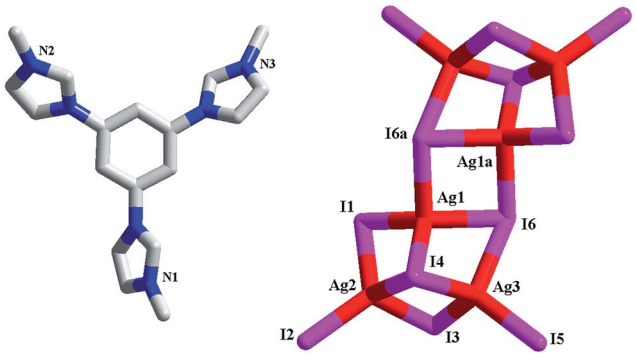

Fig. 2 Molecular structure of **2** (*a*: $-x + 2, -y + 1, -z$).

ion caps these three Ag^{+} centers, making the trinuclear cluster more stable. Note that this trinuclear cluster can be described as a incomplete cubane (lacking a tetrahedral Ag^{+} corner). Then *via* the interactions between Ag1 and I6a, two such trinuclear clusters further aggregate to form the title hexanuclear $[Ag_6I_{12}]^{6-}$ cluster. The terminal I2 and I5 are used to complete the tetrahedral coordination of Ag2 and Ag4. The shortest Ag···Ag separation in **2** is Ag1···Ag3 = 3.0833(10) Å.

$[L1]_2[Pb_3I_{12}]\cdot 2H_2O$ 3. **3** is a trinuclear iodoplumbate(II) with $L1^{3+}$ as the countercation (see Fig. 3). The asymmetric unit of **3** is found to be composed of two types of Pb^{2+} ions (Pb1, Pb2), six types of I^{-} ions (I1, I2, I3, I4, I5, I6), one $L1^{3+}$ molecules, and one lattice water molecule (Ow1). For six ions, I1, I2 and I3 adopt a terminal mode, whereas I4, I5 and I6 adopt a linear bridging mode. The Pb–I–Pb angle range is 76.83(2)–80.37(3)°. Pb1 and Pb2 are both in an octahedral site, coordinated by six I^{-} ions. The Pb–I bond length range is 3.0481(9)–3.2565(11) Å. Templated by $L1^{3+}$, Pb^{2+} and I^{-} aggregate into a trinuclear cluster. This trinuclear cluster can be described as a linear arrangement of three PbI_6 octahedra *via* sharing the face. Pb2 is located at a special position, serving as an inversion center. The contact distance between Pb1 and Pb2 is 4.174 Å. In the reported metal(II) halides (M^{2+} = Pb^{2+}, Cd^{2+}), a kind of chain structure is often observed, which can be described as a linear array of MX_6 octahedra *via* sharing the face.[15] Although the trinuclear structure in **3** is seldom found, it is actually a segment of this type of chain.

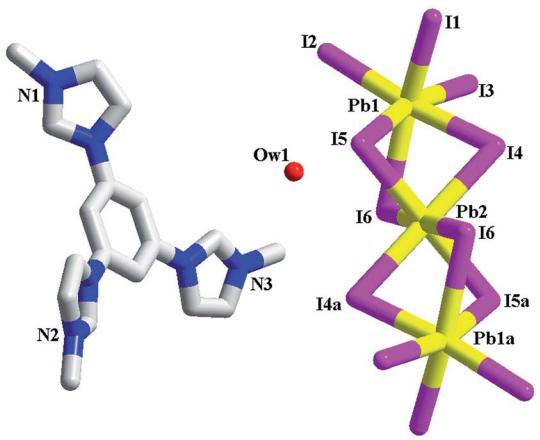

Fig. 3 Molecular structure of **3** (*a*: $-x, -y, -z + 1$).

$[L1][Bi_2I_9]$ 4. **4** is a dinuclear iodobismuthate(III) with $L1^{3+}$ as the countercation (see Fig. 4a). The asymmetric unit of **4** is found to be composed of two types of Bi^{3+} ions (Bi1, Bi2), nine types of I^{-} ions (I1–I9), and one $L1^{3+}$ cation. Although nine types of I^{-} ions are found in **4**, the inorganic anion of **4** only exhibits a simple dinuclear structure. Six I^{-} ions (I1–I3, I7–I9) act as the terminal ligands, completing the octahedral coordination of Bi1 and Bi2. The remaining three I^{-} ions (I4–I6) adopt a μ_2 coordination mode, triply bridging two Bi^{3+} centers into a dinuclear cluster. Two Bi^{3+} centers are both in an octahedral site, surrounded by six I^{-} ions. The Bi–I bond length range is 2.8692(10)–3.3736(10) Å. In fact, this dinuclear cluster can be viewed as a segment of the trinuclear cluster observed in **3**. The formation of the different cluster structures for **3** and **4** should be relative to the metal center. The difference on the charge and the size for Pb^{2+} and Bi^{3+} directly influence the formation of the cluster structures. The Bi1···Bi2 distance is 4.232 Å. In **4**, there exist the weak I···I interactions (I3···I4a = 3.997 Å, I3···I8a = 3.904 Å), *via* which, the neighboring dinuclear units are linked together into a 1-D supramolecular chain (see Fig. 4b).

Structural discussion

The title four compounds are proved to be four new organically modified iodometallate. Although the cations are all the $L1^{3+}$

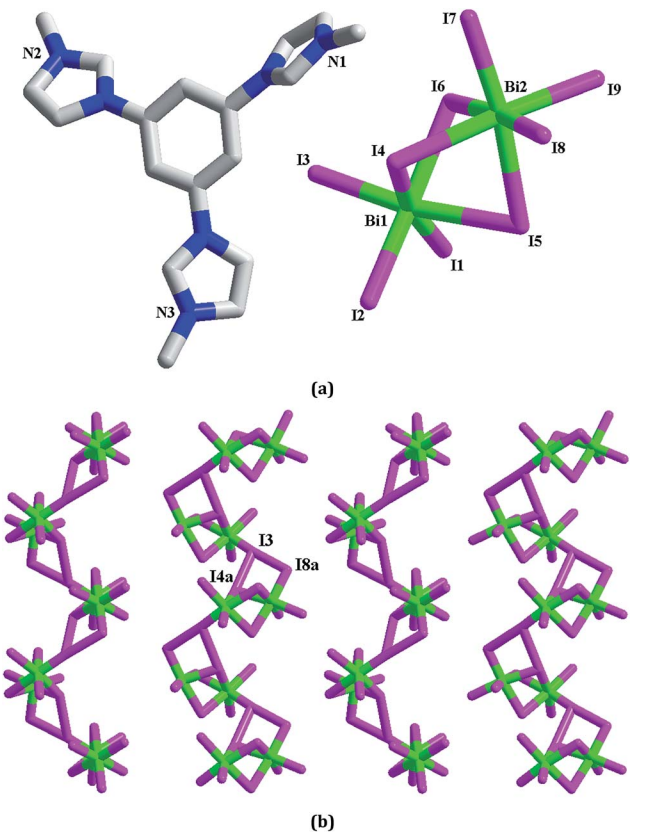

Fig. 4 Molecular structure (a) and I···I interactions between inorganic dinuclear clusters (b) in **4** (*a*: $-x + 1, y + 1/2, -z - 1/2$).

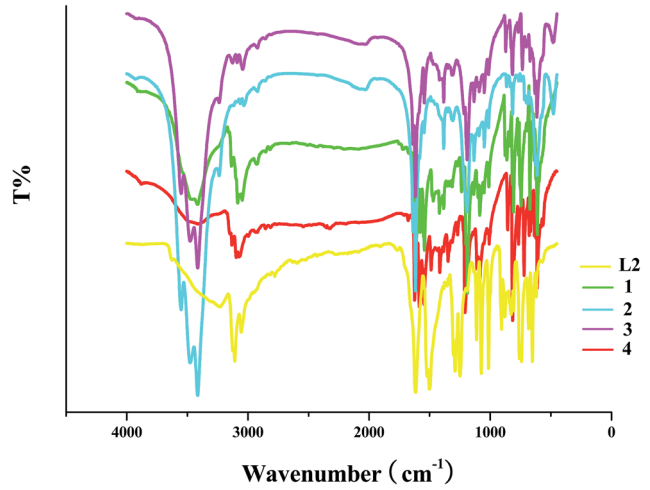

Fig. 5 IR spectra of title compounds.

molecule, the iodometallates exhibits the distinct structures. This should be mainly related to the metal center. By the size (characterized by ionic radius) and the charge, the metal center controls the structure of the iodometallate. In **1** and **2**, the iodoargentates show the different structures, which should be due to the existence of the free I^- ion in **1**. As expected, the triimidazole molecule L2 is *N*-alkylated by CH_3OH to form $L1^{3+}$.

The *N*-alkylation of the L2 molecule causes two important changes: (i) changing the size of the organic cation. The size of the organic molecule directly affects the structure of the inorganic iodometallate. In general, the larger organic cation leads to the formation of the discrete iodometallate, while the smaller organic cation corresponds to the formation of the infinite iodometallate. Although the exception is frequently observed in the reported hybrids, in the title four compounds the especial situation does not occur. With the larger $L1^{3+}$ as the counter-cation, all of the iodometallates in **1–4** display the discrete structures; (ii) changing the weak interactions between the organic molecule and inorganic anionic moiety. The N–H···X hydrogen-bonded interaction has been confirmed to play a non-ignorable role in determining the structure of inorganic anionic moiety. Once the N atom is alkylated, this kind of weak interaction will disappear.

Characterization

The obvious difference between $L1^{3+}$ and L2 is the existence of the $-CH_3$ group in the $L1^{3+}$ molecule (see Scheme 1). In the IR spectra of the as-synthesized hybrids, once the characteristic peaks of the $-CH_3$ group appear, this means that the *N*-alkylation of the L2 molecule with CH_3OH has occurred. For the $-CH_3$ group, the stretching vibration peak of C–H (ν_{C-H}) generally appears in the wavenumber range of 2925–2845 cm^{-1}, and the in-plane bending vibration peak of C–H (β_{C-H}) is

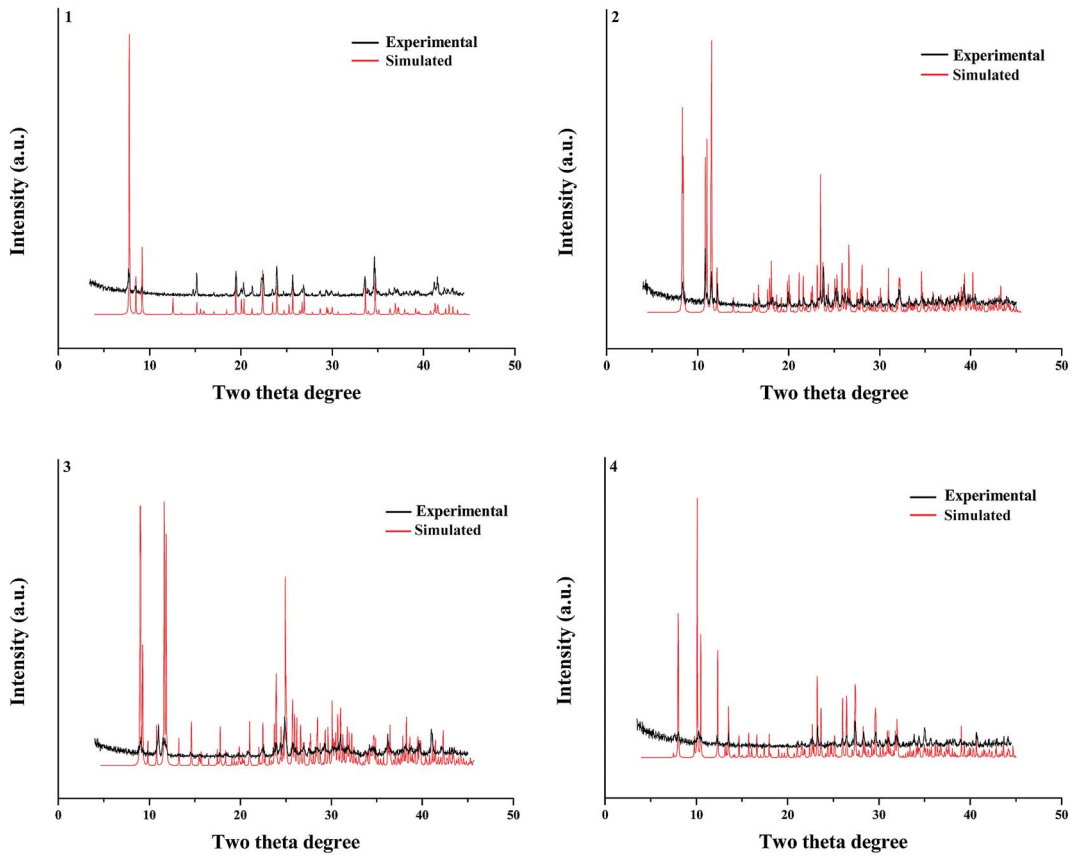

Fig. 6 Powder XRD patterns of title compounds.

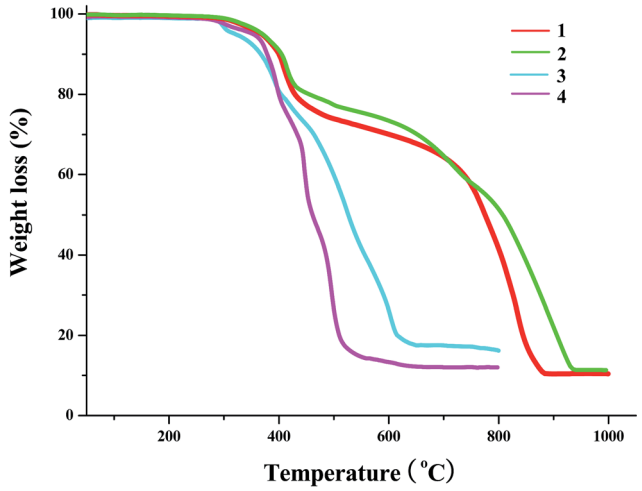

Fig. 7 TG curves of **1–4**.

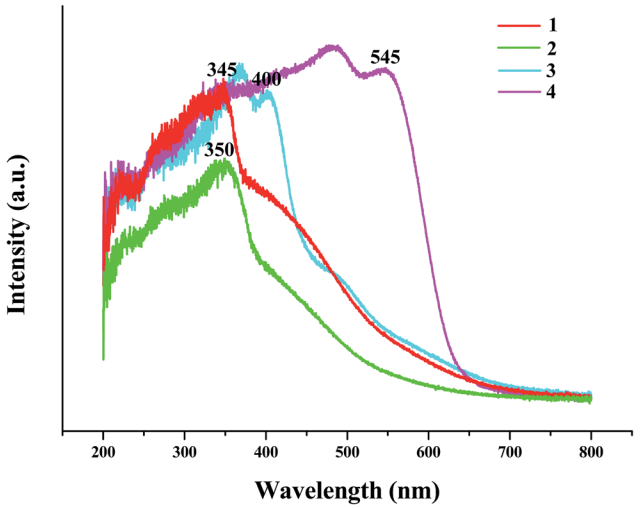

Fig. 8 Solid-state UV-vis spectra of title hybrids.

generally observed around 1380 cm^{-1}. In the IR spectra of **1–4** (see Fig. 5), these characteristic peaks are found, suggesting that L2 has been methylated by CH_3OH to form the $L1^{3+}$ molecule. $\nu_{C-H}(-CH_3)$: 2925, 2849 cm^{-1} for **1**; 2920, 2854 cm^{-1} for **2**; 2919, 2853 cm^{-1} for **3**; 2929, 2853 cm^{-1} for **4**. $\beta_{C-H}(-CH_3)$: 1419, 1386 cm^{-1} for **1**; 1386 cm^{-1} for **2**; 1386 cm^{-1} for **3**; 1418, 1385 cm^{-1} for **4**. Note that $\nu_{C-H}(-CH_3)$ is a kind of weak peak, while $\beta_{C-H}(-CH_3)$ is a kind of sharp peak. In the IR spectrum of L2, the characteristic C–H peaks for the $-CH_3$ group are not observed (also see Fig. 5). Moreover, ν_{C-H}(ring): 3086, 3051 cm^{-1} for **1**; 3063, 3034 cm^{-1} for **2**; 3091, 3043 cm^{-1} for **3**; 3100, 3071 cm^{-1} for **4**. $\nu_{C=C/C=N}$(ring): 1614, 1575, 1543 cm^{-1} for **1**; 1637, 1618 cm^{-1} for **2**; 1637, 1617, 1545 cm^{-1} for **3**; 1623, 1587, 1548 cm^{-1} for **4**. ν_{C-N}(ring): 1239, 1190 cm^{-1} for **1**; 1194, 1135 cm^{-1} for **2**; 1190, 1135 cm^{-1} for **3**; 1348, 1208, 1110, 1087 cm^{-1} for **4**. γ_{C-H}(ring; γ: out-of-plane bending vibration): 862, 809, 747 cm^{-1} for **1**; 816 cm^{-1} for **2**; 871, 818 cm^{-1} for **3**; 855, 813, 768 cm^{-1} for **4**.

Powder XRD diffraction

Fig. 6 presents the experimental and simulated powder XRD patterns of **1–4**. The experimental powder XRD pattern for each compound is in accord with the simulated one generated on the basis of structural data, confirming that the as-synthesized product is pure phase.

TG analysis

The TG behaviors of the title compounds (temperature range: 30–1000 °C for **1** and **2**; 30–800 °C for **3** and **4**) are investigated (see Fig. 7). Based on the TG curves, we can know that (i) **1**, **2** and **4** possess the better thermal stability, and can be thermal stable up to *ca.* 275 °C; (ii) two iodoargentates **1** and **2** show the similar TG behaviors. Both underwent the two steps of weight loss. The first step of weight loss (found: *ca.* 30% for **1**, *ca.* 35% for **2**) corresponds to the loss of organic cation in the form of $L1I_3$ (calcd: 31.2% for **1**, 36.4% for **2**). The second step should be a transforming process from AgI to Ag_2O. The observed residue content (*ca.* 10.6% for **1**, *ca.* 11.4% for **2**) is lower than that of the calculated (28.2% for **1**; 24.7% for **2**), suggesting that the evaporation of AgI also occurred in this step; (iii) in the temperature range of 275–800 °C, **3** and **4** only underwent the one step of weight loss. In this step, the organic cation first removed. Then PbI_2 or BiI_3 transformed into PbO or Bi_2O_3. Synchronously, part of AgI evaporated, revealed by the low residue content (found: 17.5% for **3**, 12.3% for **4**; calcd: 23.7% for **3**, 24.8% for **4**); (iii) since the content of the water molecule in **3** is minor (1.28%), it is difficult to be observed for the removal of the water molecule. Fig. S1† gives the DSC (differential scanning calorimeter) curves of **1–4**.

UV-vis spectrum analysis

The solid-state UV-vis spectra of the title compounds are also investigated. As shown in Fig. 8, the adsorption edges at 345 nm for **1**, 350 nm for **2**, 400 nm for **3**, and 545 nm for **4**, suggests that the energy gaps for four hybrids are 3.59 eV for **1**, 3.54 eV for **2**, 3.10 eV for **3**, and 2.28 eV for **4**, respectively. Compared with the energy gaps of AgI (2.81 eV),[16] PbI_2 (2.53 eV),[10d] and BiI_3 (*ca.* 1.7–2.0 eV),[17] the energy gaps for the title four hybrids all become wide (0.78 eV for **1**, 0.73 eV for **2**, 0.57 eV for **3**, and 0.28–0.58 eV for **4**), which should be due to the hybrid.

Conclusion

In summary, we employed the *in situ N*-alkylation of organic bases with alcohols to construct four new iodometallates (M^{n+} = Ag^+, Pb^{2+}, Bi^{3+}) with $L1^{3+}$ as the countercation. $L1^{3+}$ derived from the *in situ N*-alkylation of a kind of triimidazole molecule with CH_3OH. Note that the *in situ N*-alkylation of triimidazole with alcohols was investigated for the first time. Synthetically, a strong acidic environment is quite important. This chiefly affects the formation of the important intermediate CH_3I. The *N*-methylation of L2 not only changes the size of the organic cation, but also makes another potential factor in influencing the cluster structure (N–H···I hydrogen bond) disappear. With the large bulk $L1^{3+}$ as the counteraction, the inorganic anionic

moieties all show the discrete structures. By the size and the charge, the metal center controls the structure of the inorganic anionic cluster. The incorporated I^- anion also plays a key role in controlling the cluster structure. Based on the IR spectrum, we can preliminarily judge whether the triimidazole molecule has been *N*-alkylated by alcohols. The UV-vis spectrum analysis indicates the energy gaps of the title four hybrids.

Acknowledgements

This research was supported by the National Natural Science Foundation of China (No. 21271083).

References

1 (*a*) X. M. Zhang, *Coord. Chem. Rev.*, 2005, **249**, 1201–1219; (*b*) X. M. Chen and M. L. Tong, *Acc. Chem. Res.*, 2007, **40**, 162–170; (*c*) H. Zhao, Z. R. Qu, H. Y. Ye and R. G. Xiong, *Chem. Soc. Rev.*, 2008, **37**, 84–100; (*d*) H. B. Zhu and S. H. Gou, *Coord. Chem. Rev.*, 2011, **255**, 318–338.

2 (*a*) D. C. Zhong, Y. Q. Wen, J. H. Deng, X. Z. Luo, Y. N. Gong and T. B. Lu, *Angew. Chem., Int. Ed.*, 2015, **54**, 11795–11799; (*b*) Y. Z. Tang, J. B. Xiong, J. X. Gao, Y. H. Tan, Q. Xu and H. R. Wen, *Inorg. Chem.*, 2015, **54**, 5462–5466; (*c*) T. Wen, D. X. Zhang, Q. R. Ding, H. B. Zhang and J. Zhang, *Inorg. Chem. Front.*, 2014, **1**, 389–392; (*d*) J. D. Tsai and C. I. Yang, *Dalton Trans.*, 2014, **43**, 15576–15582; (*e*) Z. F. Liu, M. F. Wu, F. K. Zheng, S. H. Wang, J. Xiao, G. C. Guo and A. Q. Wu, *CrystEngComm*, 2013, **15**, 7038–7047; (*f*) T. Jin, F. Kitahara, S. Kamijo and Y. Yamamoto, *Chem.–Asian J.*, 2008, **3**, 1575–1580; (*g*) X. M. Zhang, Y. F. Zhao, H. S. Wu, S. R. Batten and S. W. Ng, *Dalton Trans.*, 2006, 3170–3178.

3 (*a*) X. M. Zhang, M. L. Tong and X. M. Chen, *Angew. Chem., Int. Ed.*, 2002, **41**, 1029–1031; (*b*) X. M. Zhang, M. L. Tong, M. L. Gong, H. K. Lee, L. Luo, K. F. Li, Y. X. Tong and X. M. Chen, *Chem.–Eur. J.*, 2002, **8**, 3187–3194; (*c*) S. L. Zheng, J. P. Zhang, W. T. Wong and X. M. Chen, *J. Am. Chem. Soc.*, 2003, **125**, 6882–6883; (*d*) J. Tao, Y. Zhang, M. L. Tong, X. M. Chen, T. Yuen, C. L. Lin, X. Y. Huang and J. Li, *Chem. Commun.*, 2002, 1342–1343.

4 (*a*) A. J. Black, N. R. Champness, S. S. M. Chung, W. S. Li and M. Schröder, *Chem. Commun.*, 1997, 1675–1676; (*b*) C. M. Liu, S. Gao and H. Z. Kou, *Chem. Commun.*, 2001, 1670–1671; (*c*) N. Zheng, X. Bu and P. Feng, *J. Am. Chem. Soc.*, 2002, **124**, 9688–9689; (*d*) O. R. Evens and W. Lin, *Cryst. Growth Des.*, 2001, **1**, 9–11; (*e*) Q. H. Wei, L. Y. Zhang, G. Q. Yin, L. X. Shi and Z. N. Chen, *J. Am. Chem. Soc.*, 2004, **126**, 9940–9941; (*f*) J. Zhang, T. Wu, P. Y. Feng and X. H. Bu, *Chem. Mater.*, 2008, **20**, 5457–5459.

5 (*a*) X. X. Hu, J. Q. Xu, P. Cheng, X. Y. Chen, X. B. Cui, J. F. Song, G. D. Yang and T. G. Wang, *Inorg. Chem.*, 2004, **43**, 2261–2266; (*b*) Y. N. Wang, Q. S. Huo, P. Zhang, J. H. Yu and J. Q. Xu, *Spectrochim. Acta, Part A*, 2016, **167**, 33–40; (*c*) J. H. Yu, Y. C. Zhu, D. Wu, Y. Yu, Q. Hou and J. Q. Xu, *Dalton Trans.*, 2009, 8248–8256; (*d*) Y. N. Wang, G. H. Li, F. Q. Bai, J. H. Yu and J. Q. Xu, *Dalton Trans.*, 2014, **43**, 15617–15627; (*e*) J. Jin, F. Q. Bai, M. J. Jia, Y. Peng, J. H. Yu and J. Q. Xu, *Dalton Trans.*, 2012, **41**, 2382–2392; (*f*) Y. N. Wang, Q. F. Yang, G. H. Li, P. Zhang, J. H. Yu and J. Q. Xu, *Dalton Trans.*, 2014, **43**, 11646–11657; (*g*) Y. N. Wang, J. H. Yu and J. Q. Xu, *Inorg. Chem. Front.*, 2014, **1**, 673–681; (*h*) Y. N. Wang, J. H. Yu and J. Q. Xu, *Polyhedron*, 2014, **83**, 220–227.

6 (*a*) C. Feng, D. Zhang, Z. Chu and H. Zhao, *Polyhedron*, 2016, **115**, 288–296; (*b*) Y. W. Li, H. Y. Ma, S. N. Wang, J. Xu, D. C. Li, J. M. Dou and X. H. Bu, *RSC Adv.*, 2015, **5**, 88809–88815; (*c*) H. L. Jia, Z. Shi, Q. F. Yang, J. H. Yu and J. Q. Xu, *Dalton Trans.*, 2014, **43**, 5806–5814; (*d*) R. Sultana, T. S. Lobana and A. Castineriras, *RSC Adv.*, 2015, **5**, 100579–100588; (*e*) S. Zou, Q. Li and S. Du, *RSC Adv.*, 2015, **5**, 34936–34941; (*f*) X. Hang, S. Wang, X. Zhu, H. Han and W. Liao, *CrystEngComm*, 2016, **18**, 4938–4943; (*g*) R. Y. Huang, H. Jiang, C. H. Zhu and H. Xu, *RSC Adv.*, 2016, **6**, 3341–3349; (*h*) L. Fan, L. Li, B. Xu, M. Qian, J. Li and H. Hou, *Inorg. Chim. Acta*, 2014, **423**, 46–51; (*i*) B. Ji, D. Deng, J. Ma, C. Sun and B. Zhao, *RSC Adv.*, 2015, **5**, 2239–2248; (*j*) H. Zhao, S. Y. Zhou, C. Feng, N. X. Wei and G. G. Wang, *Inorg. Chim. Acta*, 2014, **421**, 169–175; (*k*) D. C. Zhong, H. B. Guo, J. H. Deng, Q. Chen and X. Z. Luo, *CrystEngComm*, 2015, **17**, 3519–3525; (*l*) Y. W. Li, Y. Tao and T. L. Hu, *Solid State Sci.*, 2012, **14**, 1117–1125; (*m*) C. Xu, L. Li, Y. Wang, Q. Guo, X. Wang, H. Hou and Y. Fan, *Cryst. Growth Des.*, 2011, **11**, 4667–4675; (*n*) S. R. Zheng, S. L. Cai, J. Fan, T. T. Xiao and W. G. Zhang, *Inorg. Chem. Commun.*, 2011, **14**, 1097–1101; (*o*) C. C. Ji, J. Li, Y. Z. Li, Z. J. Guo and H. G. Zheng, *CrystEngComm*, 2011, **13**, 459–466.

7 J. K. Cheng, Y. G. Yao, J. Zhang, Z. J. Li, Z. W. Cai, X. Y. Zhang, Z. N. Chen, Y. B. Chen, Y. Kang, Y. Y. Qin and Y. H. Wen, *J. Am. Chem. Soc.*, 2004, **126**, 7796–7797.

8 (*a*) B. Xin, Y. Li, G. Zeng, Y. Peng, G. Li, Z. Shi and S. Feng, *Z. Anorg. Allg. Chem.*, 2013, **639**, 611–617; (*b*) G. N. Niu, J. R. Shi, X. J. Han, X. Zhang, K. Li, J. Li, T. Zhang, Q. S. Liu, Z. W. Zhang and C. Li, *Dalton Trans.*, 2015, **44**, 12561–12575; (*c*) J. Wu, Y. Yan, B. Liu, X. Wang, J. Li and J. Yu, *Chem. Commun.*, 2013, **49**, 4995–4997; (*d*) G. Zeng, S. Xing, X. Han, B. Xin, Y. Yang, X. Wang, G. Li, Z. Shi and S. Feng, *RSC Adv.*, 2015, **5**, 40792–40797; (*e*) C. Zhang, J. Shen, Q. Guan, T. Yu and Y. Fu, *Solid State Sci.*, 2015, **46**, 14–18; (*f*) G. N. Liu, L. L. Liu, Y. N. Chu, Y. Q. Sun, Z. W. Zhang and C. Li, *Eur. J. Inorg. Chem.*, 2015, 478–487; (*g*) G. N. Liu, X. M. Jiang, Q. S. Fan, M. B. Hussain, K. Li, H. Sun, X. Y. Li, W. Q. Liu and C. Li, *Inorg. Chem.*, 2017, **56**, 1906–1918; (*h*) T. Yu, L. An, L. Zhang, J. Shen, Y. Fu and Y. Fu, *Cryst. Growth Des.*, 2014, **14**, 3875–3879; (*i*) J. Shen, C. Zhang, T. Yu, L. An and Y. Fu, *Cryst. Growth Des.*, 2014, **14**, 6337–6342.

9 (*a*) J. Y. Xue, J. C. Li, H. X. Li, H. Y. Li and J. P. Lang, *Tetrahedron*, 2016, **72**, 7014–7020; (*b*) H. Chan, Y. Chen, M. Dai, C. N. Lü, H. F. Wang, Z. G. Ren, Z. J. Huang, C. Y. Ni and J. P. Lang, *CrystEngComm*, 2012, **14**, 466–473; (*c*) Y. Chen, Z. Yang, C. X. Guo, C. Y. Ni, H. X. Li, Z. G. Ren and J. P. Lang, *CrystEngComm*, 2011, **13**, 243–250; (*d*) Y. Chen, Z. Yang, C. X. Guo, C. Y. Ni, Z. G. Ren, H. X. Li and J. P. Lang, *Eur. J. Inorg. Chem.*, 2010, 5326–5333.

10 (*a*) G. E. Wang, M. S. Wang, X. M. Jiang, Z. F. Liu, R. G. Lin, L. Z. Cai, G. C. Guo and J. S. Huang, *Inorg. Chem. Commun.*, 2011, **14**, 1957–1961; (*b*) G. E. Wang, X. M. Jiang, M. J. Zhang, H. F. Chen, B. W. Liu, M. S. Wang and G. C. Guo, *CrystEngComm*, 2013, **15**, 10399–10404; (*c*) G. E. Wang, G. Xu, M. S. Wang, L. Z. Cai, W. H. Li and G. C. Guo, *Chem. Sci.*, 2015, **6**, 7222–7226; (*d*) Z. J. Zhang, S. C. Xiang, G. C. Guo, G. Xu, M. S. Wang, J. P. Zou, S. P. Guo and J. S. Huang, *Angew. Chem., Int. Ed.*, 2008, **47**, 4149–4152; (*e*) G. E. Wang, G. Xu, B. W. Liu, M. S. Wang, M. S. Yao and G. C. Guo, *Angew. Chem., Int. Ed.*, 2016, **55**, 514–518.

11 (*a*) J. J. Hou, C. H. Guo and X. M. Zhang, *Inorg. Chim. Acta*, 2006, **359**, 3991–3995; (*b*) J. J. Hou, S. L. Li, C. R. Li and X. M. Zhang, *Dalton Trans.*, 2010, **39**, 2701–2707; (*c*) S. L. Li and X. M. Zhang, *Inorg. Chem.*, 2014, **53**, 8376–8383.

12 (*a*) G. M. Wang, J. Q. Jiao, X. Zhang, X. M. Zhao, X. Yin, Z. H. Wang, Y. X. Wang and J. H. Lin, *Inorg. Chem. Commun.*, 2014, **39**, 94–98; (*b*) G. M. Wang, J. H. Lin, J. Q. Jiao, X. Zhang, X. M. Zhao, X. Yin, J. S. Huang, Y. X. Wang and J. H. Lin, *Inorg. Chem. Commun.*, 2014, **43**, 105–109; (*c*) G. M. Wang, J. H. Li, X. Zhang, J. Q. Jiao, Z. Z. Bao, X. M. Zhao, W. W. Jiang, Y. X. Wang and J. H. Lin, *Inorg. Chem. Commun.*, 2014, **46**, 295–300; (*d*) G. Wang, Z. Ding, J. Li, X. Lv, X. Zhang, X. Zhao, Z. Wang, Y. Wang and J. Lin, *CrystEngComm*, 2014, **16**, 3296–3304; (*e*) G. Wang, J. Li, X. Zhang, P. Wang, B. B. Pang, Z. Wang, Y. Wang, J. Lin and C. Pan, *Dalton Trans.*, 2013, **42**, 13084–13091; (*f*) G. M. Wang, J. H. Li, L. Wei, X. Zhang and Z. Z. Bao, *RSC Adv.*, 2016, **5**, 74811–74820.

13 (*a*) Q. Hou, F. Q. Bai, M. J. Jia, J. Jin, J. H. Yu and J. Q. Xu, *CrystEngComm*, 2012, **14**, 4000–4007; (*b*) J. J. Zhao, X. Zhang, Y. N. Wang, H. L. Jia, J. H. Yu and J. Q. Xu, *J. Solid State Chem.*, 2013, **207**, 152–157; (*c*) Q. Hou, J. J. Zhao, T. Q. Zhao, J. Jin, J. H. Yu and J. Q. Xu, *J. Solid State Chem.*, 2011, **184**, 1756–1760; (*d*) Q. Hou, J. N. Xu, J. H. Yu, T. G. Wang, Q. F. Yang and J. Q. Xu, *J. Solid State Chem.*, 2010, **183**, 1561–1566.

14 G. M. Sheldrick, *Acta Crystallogr., Sect. A: Found. Crystallogr.*, 2008, **64**, 112–122.

15 (*a*) B. Guo, X. Zhang, Y. N. Wang, J. J. Huang, J. H. Yu and J. Q. Xu, *Dalton Trans.*, 2015, **44**, 5095–5105; (*b*) G. Q. Mei and W. Q. Liao, *J. Mater. Chem. C*, 2015, **3**, 8535–8541; (*c*) Y. J. She, S. P. Zhao, Z. F. Tian and X. M. Ren, *Inorg. Chem. Commun.*, 2014, **46**, 29–32; (*d*) S. Eppel, N. Fridman and G. Frey, *Cryst. Growth Des.*, 2015, **15**, 4363–4371; (*e*) H. H. Li, Z. R. Chen, L. C. Cheng, Y. J. Wang, M. Feng and M. Wang, *Dalton Trans.*, 2010, **39**, 11000–11007; (*f*) J. J. Liu, Y. F. Guan, C. Jiao, M. J. Lin, C. C. Huang and W. X. Dai, *Dalton Trans.*, 2015, **44**, 5957–5960; (*g*) C. H. Wang, H. J. Du, Y. Li, Y. Y. Niu and H. W. Hou, *New J. Chem.*, 2015, **39**, 7372–7378; (*h*) H. L. Jia, G. H. Li, H. Ding, Z. M. Gao, G. Zeng, J. H. Yu and J. Q. Xu, *RSC Adv.*, 2013, **3**, 16416–16425.

16 (*a*) T. Yu, Y. Fu, Y. Wang, P. Hao, J. Shen and Y. Fu, *CrystEngComm*, 2015, **17**, 8752–8761; (*b*) T. L. Yu, P. F. Hao, J. J. Shen, H. H. Li and Y. L. Fu, *Dalton Trans.*, 2016, **45**, 16505–16510; (*c*) C. Zhang, J. Shen, Q. Guan, T. Yu and Y. Fu, *Solid State Sci.*, 2015, **46**, 14–18.

17 (*a*) A. M. Goforth, M. A. Tershansy, M. D. Smith, L. Peterson Jr, J. G. Kelley, W. J. I. DeBenedetti and H.-Z. zur Loye, *J. Am. Chem. Soc.*, 2011, **133**, 603–612; (*b*) L. M. Wu, X. T. Wu and L. Chen, *Coord. Chem. Rev.*, 2009, **253**, 2787–2804; (*c*) J. Heine, *Dalton Trans.*, 2015, **44**, 10069–10077.